J. Condensed Matter Nucl. Sci. 4 (2011) 69–80

Research Article

Absorption Capacity and Heat Evolution with Loading of Hydrogen Isotope Gases for Pd Nanopowder and Pd/Ceramics Nanocomposite

T. Hioki *, H. Azuma, T. Nishi, A. Itoh, S. Hibi, J. Gao and T. Motohiro

Toyota Central Research and Development Laboratories Inc., Nagakute, Aichi 480-1192, Japan

J. Kasagi

Research Center for Electron Photon Science, Tohoku University, Sendai 982-0826, Japan

Abstract

Using Sievert's method, the hydrogen (/deuterium) absorption capacity was measured for Pd nanopowder with particle size 10–20 nm and for Pd-γAl_2O_3 nanocomposites with Pd particle size 2–5 nm. In order to eliminate the influence of oxidized Pd particles on the absorption capacity, measurements were repeated three or four times without exposing the samples to air. For both nano-Pd materials, the absorption capacity at 1MPa was found to be slightly smaller than that of Pd bulk. The difference in the absorption capacity between hydrogen and deuterium, i.e., the isotope effect, was negligible within the experimental error. It was found that the average size of the Pd particles was significantly increased after the repeated measurements of the absorption capacity. The heat generated upon pressurizing the materials with deuterium or hydrogen up to 1MPa was measured using a flow calorimeter. Similar to the measurements of absorption capacity, the heat measurements were also conducted repeatedly. The observed heat generation was composed of two stages, i.e., the first stage during pressurizing the samples from 0 to 1 MPa and the second stage, where the sample was kept under a fixed pressure of 1 MPa. The heat generated in the first stage was much larger at the time of the first measurement than at the second or third. The heat generated in the first stage was largely explained by taking into account two chemical reactions, i.e., the water formation reaction and the deuteride formation reaction. It was noted that in the second stage, where the heat generated from chemical reactions was hardly expected to occur, a small heat power was observed intermittently. This heat evolution was observed frequently when the samples were loaded with deuterium.

Keywords: Calorimeter, CMNS, Deuterium absorption, Heat evolution, Hydrogen storage, Pd nanoparticle

PACS: 25.45.-z, 65.80.-g, 81.07.Bc, 81.07.Wx, 88.30.R-

*E-mail: hioki@mosk.tytlabs.co.jp

1. Introduction

It has recently been recognized that nanometer scale structures of Pd or nanometer size Pd particles are essential to successfully observe low energy nuclear phenomena in condensed matter. Iwamura et al. have used nanometer-size multi-layers of CaO and Pd and have reported an observation of nuclear transmutation from Sr to Mo and Cs to Pr, as a result of deuterium permeation through the multi-layer structure [1]. Dardik et al. have achieved a high reproducibility of excess heat generation by using the ultrasonically excited "Super Wave" electrolysis technique [2]. In their experiments, a high deuterium loading has been obtained, i.e., D/Pd, the number of absorbed deuterium atoms to Pd atoms, is larger than 0.95. The remarkable increase in the deuterium loading has been attributed to increasing the surface area of the Pd cathode as well as cleaning and activating the cathode surface as a result of the ultrasonic excitation [2]. It has long been known that attaining a D/Pd ratio larger than 0.88 is favorable to observe excess heat in electrochemical loading of Pd with deuterium [3].

Arata and Zhang have recently reported that by simply loading a nano-Pd–ZrO_2 system with deuterium gas, heat generation due to a nuclear reaction is observed [4]. They have also observed a remarkable increase of ^{4}He in the gas sampled from the powder after the loading experiments, suggesting that the heat is generated as a result of the D–D nuclear reaction that yields ^{4}He as ash. For nano-Pd–ZrO_2 systems, a high value of H/Pd has been reported and attributed to interfacial hydrogen spillover effect [5]. Kitamura et al. have constructed a twin type flow calorimeter system to quantitatively evaluate the heat reported by Arata and Zhang, and have observed anomalously large energies of hydrogen isotope gas absorption as well as large D/Pd and H/Pd ratios of about 1.1 [6].

In this study, in order to clarify the relationship between Pd particle size and hydrogen (/deuterium) absorption capacity, the volumetric method or Sievert's method was employed and the pressure-composition isotherms were measured for Pd nanopowder and nanoPd-γAl_2O_3composites. A flow calorimeter was constructed and used to evaluate the heat generated upon pressurizing the materials with hydrogen isotope gases. In order to identify the properties of metallic Pd nanoparticles, efforts were made to separate the influences of oxidized Pd on the absorption capacity and heat evolution, i.e., both quantities were measured repeatedly three or four times, without exposing the samples to air. Prior to each cycle of measurement, the samples were heat treated in vacuum to remove the adsorbed molecules or to completely eliminate the hydrogen or deuterium absorbed in the preceding measurement. The degree of oxidation of Pd nanoparticles was estimated from the results of the repeated measurements of the absorption capacity and was used to evaluate the heat generated from chemical reactions.

2. Experimental

2.1. Materials

The materials were Pd nanopowder and Pd nanocomposite. The Pd nanopowder (^{TM}AY4030) was commercially obtained from Tanaka Kikinzoku Kogyo. The Pd-γAl_2O_3composites with Pd concentrations of 13 and 20 wt% were prepared by impregnating the γAl_2O_3 support of specific surface area 90 m^2/g with an aqueous solution of $Pd(NO_3)_2$, followed by drying in the ambient atmosphere and subsequent heating at 773 K for 2 h in the air. By transmission electron microscopy (TEM) observation, the size of the Pd (/PdO) particles was determined to be 10–20 and 2–5 nm for the Pd nanopowder and the nanoPd-γAl_2O_3 composites, respectively.

2.2. Hydrogen/deuterium storage capacity

The hydrogen (/deuterium) absorption behavior up to 1 MPa was investigated using a pressure-composition isotherm apparatus (Suzuki Shokan Co. Ltd.). The amount of the measured samples was about 3g of Pd. The purity of hydrogen and deuterium gases was 99.99999% and 99.995%, respectively.

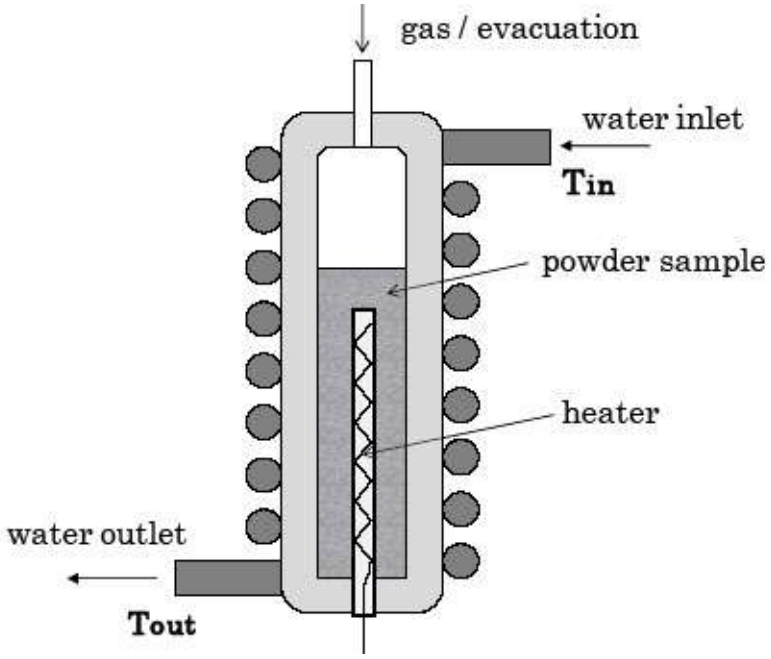

Figure 1. Schematic of the calorimeter.

2.3. Calorimetry

A flow calorimeter was constructed and used to measure the heat evolution upon pressurizing the samples with hydrogen isotope gases. A schematic of the calorimeter is shown in Fig. 1. Thermocouples of alumel–chromel were used to measure the temperature difference, T_{out}–T_{in}, between the inlet and outlet of the cooling water. The flow rate of water, f, was measured using a Coriolis force-type flow meter.

The temperature difference and the flow rate of water were registered every 30 s, and used to calculate the heat power P_{out}, following the equation,

$$P_{out} = C(T_{out} - T_{in})\, f/r, \tag{1}$$

where C is the specific heat of water and r the recovery rate of heat. An electric heater was mounted at the center of the sample vessel. The value of r was determined experimentally so that P_{out} was equal to the electric input power P_{in} under conditions where no heat source other than the electric heater existed. The value of r was almost independent of the species of the used gas (H_2, D_2 and He), the gas pressure of 0–1 MPa, and the value of P_{in} in the range of 1–5 W. It was dependent on the flow rate of water. An example of r as a function of f is shown in Fig. 2, where the sample vessel was mounted with Pd nanopowder of 26 g and pressurized with He of 0.85 MPa. In the present study, r was fixed to be 55%, because f used in this study was 6–7 ml/min. The fluctuation and the drift of the measured output power were examined under a condition where Pd powder of 26 g was loaded with He up to 1 MPa. The result is shown in Fig. 3. In order to suppress the drift, the calorimeter system was thermally insulated from the ambient atmosphere. The accuracy of the calorimeter was ±50 mW. The gases were supplied into the sample vessel through a needle valve and a mass flow controller. The flow rate of gas was about 20 ml/min.

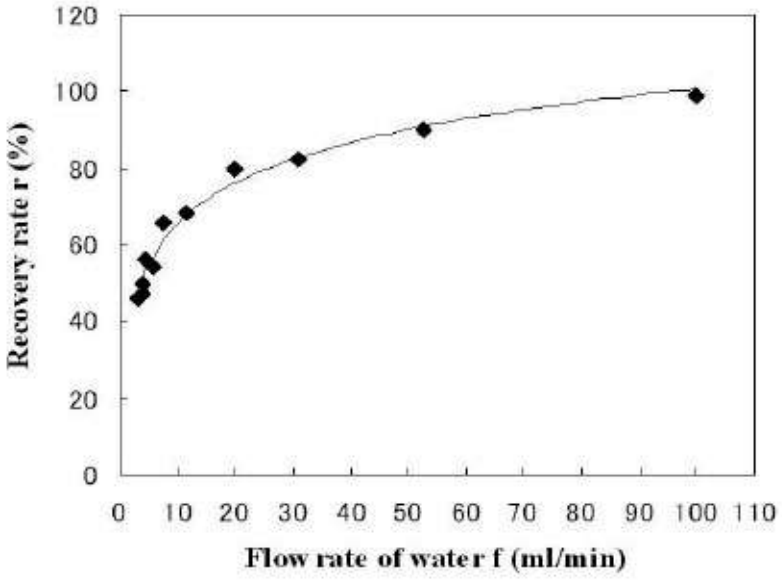

Figure 2. Recovery rate (r) as a function of flow rate (f) for Pd nanopowder AY4030 of 26 g under a He gas pressure of 0.85 MPa. The electric input power was 1.5 W or 0.66 W. The solid line is drawn to connect the data points smoothly.

3. Results and Discussion

3.1. Deuterium/hydrogen storage capacity

Pressure-composition (PC) isotherms at 300 K for Pd nanopowder AY4030 and 13 wt%Pd-γAl_2O_3 composite are shown in Figs. 4 and 5, respectively. The measurements were conducted four times repeatedly. The first, second, and

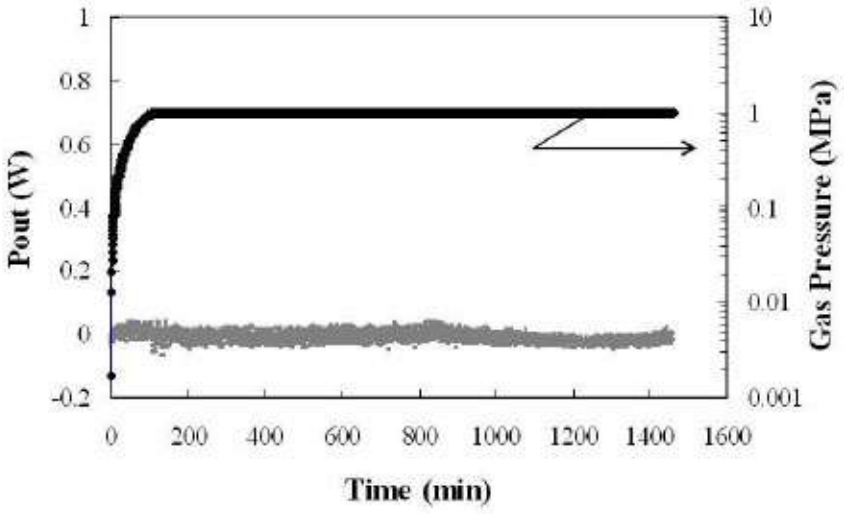

Figure 3. Output power and He gas pressure as a function of time for Pd nanopowder of 26 g.

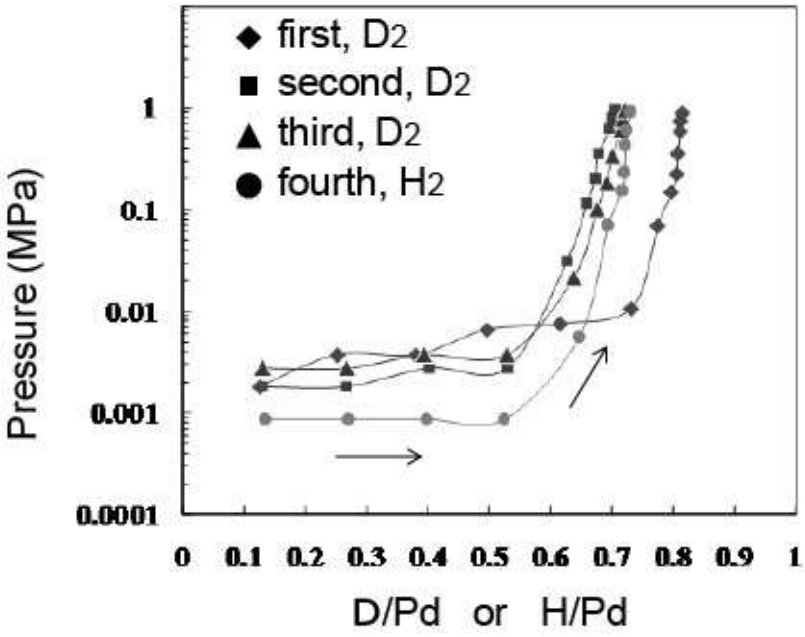

Figure 4. PC isotherms of Pd nanoparticles AY4030. Isotherms were measured four times repeatedly. The arrows show the sequence of the measurements.

third loadings were with deuterium gas and the fourth loading was with hydrogen gas. Prior to each measurement, the sample was heated in vacuum at 523 K for 2 h in order to remove adsorbed molecules (first) or to completely remove the deuterium absorbed in the preceding measurement (second, third, and fourth).

It is seen in Fig. 4 that the apparent D/Pd value at 1 MPa for the first measurement is 0.82. This value is considerably larger than those of the second (0.69) and the third (0.70) measurements. This difference is attributed to the fact that in the first measurement, the surface layer of Pd particles is initially oxidized and this oxide layer is reduced to metallic Pd during the first time loading with deuterium gas. From the measured difference, the number of Pd atoms in the form of PdO for the as-received powder is estimated to be about 6 at.% to the total number of Pd atoms.

The difference in the apparent absorption capacity between the first and second measurements is much more remarkable for the composite sample, as seen in Fig. 5. The apparent D/Pd value at 1 MPa in the first loading with D_2 is 2.7, while the values in the second and third loadings are about 0.71. The apparent D/Pd value of 2.7 in the first measurement is understood if we assume that all the Pd in the sample is oxidized, i.e., in the chemical state of PdO. Then, if the sample is exposed to deuterium or hydrogen, the following water formation reaction and deuteride (/hydride) formation reaction will proceed.

$$\mathrm{PdO} + \mathrm{D_2} \rightarrow \mathrm{Pd} + \mathrm{D_2O} + \Delta\mathrm{H(water)}, \tag{2}$$

$$\mathrm{Pd} + (1/2)(\mathrm{D/Pd})\mathrm{D_2} \rightarrow \mathrm{PdD_{(D/Pd)}} + \Delta\mathrm{H(deuteride)}. \tag{3}$$

Reaction (2) gives an apparent D/Pd value of 2, while reaction (3) gives the true value of D/Pd. In the second and third loadings, only reaction (3) is expected to occur, and D/Pd for this sample is 0.71 from the experiment. Because both reactions (2) and (3) occur in the first loading, an apparent D/Pd value of about 2.7 should be obtained.

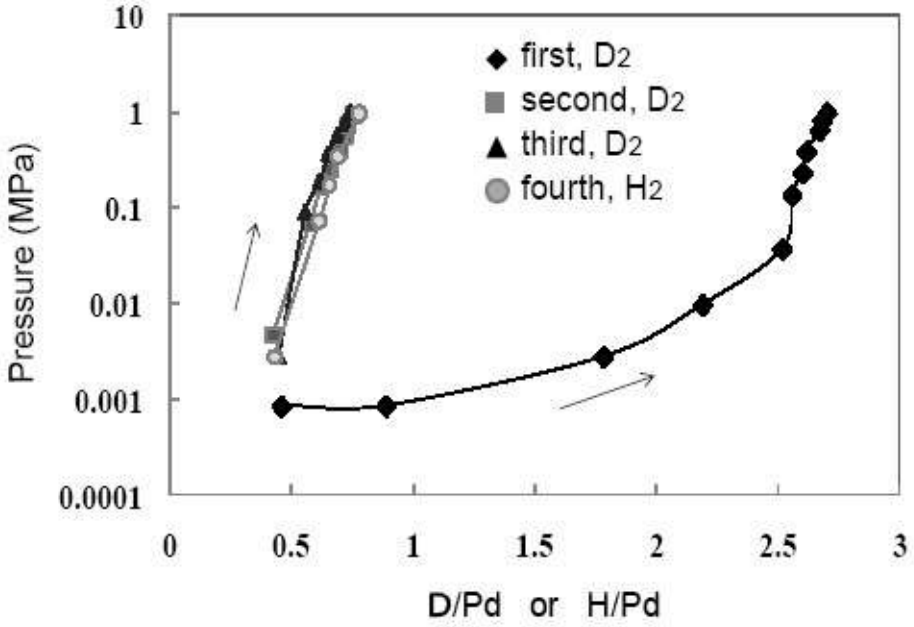

Figure 5. PC isotherms of 13 wt.%Pd-γAl_2O_3. Isotherms were measured four times repeatedly. The arrows show the sequence of the measurements.

In order to confirm the chemical composition of the sample, the X-ray diffraction pattern was taken for 13 wt.%Pd-γAl_2O_3 after the heat treatment in vacuum at 523 K for 2 h. The diffraction pattern clearly showed that the sample consisted of PdO and γAl_2O_3, while the diffraction pattern for the sample after the four-fold PC measurements showed that the sample consisted of metallic Pd and γAl_2O_3. In Table 1, the results of the absorption capacity at 1 MPa are summarized.

PC isotherms were also measured three times with hydrogen gas for 13 wt.%Pd- and 20 wt.%Pd-γAl_2O_3 and for Pd bulk in the form of a 0.1 mm thick-foil. The results are summarized in Table 2.

As seen in Table 2, large differences in the absorption capacity between the first and the second loading with hydrogen are observed for the two composite samples, whereas no difference for the Pd foil can be seen. The absorption capacity for the foil sample agrees well with the literature value for Pd bulk [7].

From these results, it has been demonstrated that the PdO in the Pd nanopowder and nanocomposites easily reduces to metallic Pd, once it is exposed to deuterium or hydrogen. In the second, third, and fourth loadings, the measured values of absorption capacity are for metallic Pd particles. It is seen from Table 1 that the deuterium absorption capacity of Pd nanopowder AY4030 is almost the same as that of 13 wt.%Pd-γAl_2O_3. It is also seen that the value of H/Pd at the fourth measurement almost agrees with the D/Pd value in the second or third measurement for both the Pd powder

Table 1. The order of measurement cycles and D/Pd (or H/Pd) at 300 K under 1 MPa.

	First (D_2)	Second (D_2)	Third (D_2)	Fourth (H_2)
nanoPd (AY4030)	0.82±0.02	0.69±0.02	0.70±0.02	0.71±0.02
13 wt.%Pd-Al_2O_3	2.7±0.2	0.71±0.02	0.72±0.02	0.72±0.02

Table 2. The order of measurement cycle and H/Pd at 300 K under 1 MPa.

	First (H_2)	Second (H_2)	Third (H_2)
13 wt.%Pd-Al_2O_3	2.8±0.2	0.69±0.02	0.71±0.02
20 w.t%Pd-Al_2O_3	2.4±0.2	0.68±0.02	0.70±0.02
Pd bulk (foil)	0.74±0.02	0.74±0.02	0.74±0.02

and the composite sample. Therefore, the isotope effect of these materials is negligible within the experimental error, as far as the absorption capacity at 1 MPa is concerned. Furthermore, it is noted from Tables 1 and 2 that the hydrogen absorption capacity for all the nanoPd materials used in the present study is slightly smaller compared to the value of Pd bulk.

Figure 6 compares the TEM images for the as-received Pd powder AY-4030 and the powder after the four cyclic measurements of absorption capacity. The average size of the Pd particles is initially 10–20 nm, whereas that of the Pd particles after the measurements is about 50 nm. The local temperature at the contact point of assembling Pd particles will rise significantly with the heat of reaction (2) and/or (3). This local temperature rise may cause the observed growth of the Pd particles.

Similar growth of Pd nanoparticles is also observed for the composite sample, as shown in Fig. 7. The size of PdO for the as-synthesized 13 wt.%Pd-γAl_2O_3 is 2–5 nm, whereas the size of Pd particles after the four cyclic measurements of absorption capacity is 2–15 nm. Therefore, the growth of Pd particles in the nanocomposite material is suppressed compared to that in the Pd nanopowder, although the heat generated with the loading of hydrogen or deuterium is much larger for the nearly 100% oxidized Pd particles of the composite, as described later. In the composite sample, Pd particles of the smallest size i.e., 2 nm, are still observed after the exposure to deuterium and hydrogen. It is probable that the Pd particles formed in the pores of γAl_2O_3 are hard to grow owing to the separation of Pd particles by the wall of Al_2O_3.

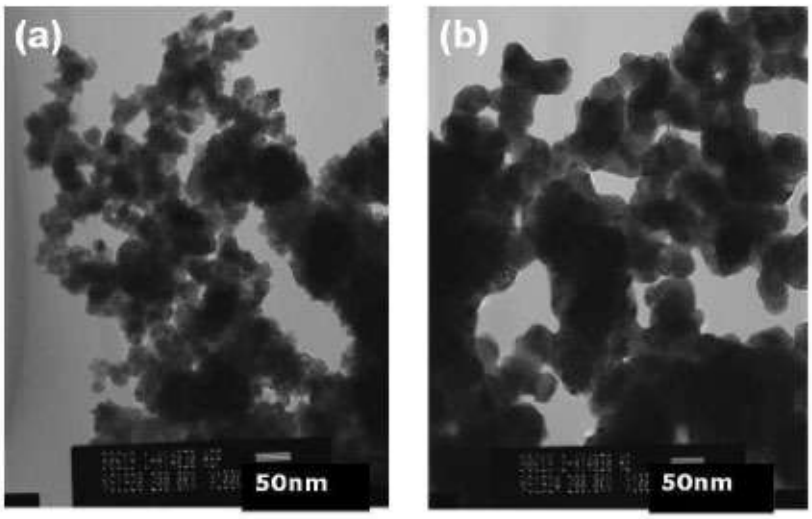

Figure 6. TEM images of Pd nanopowder AY4030; (a) as-received, (b) after four cycle measurements of absorption capacity.

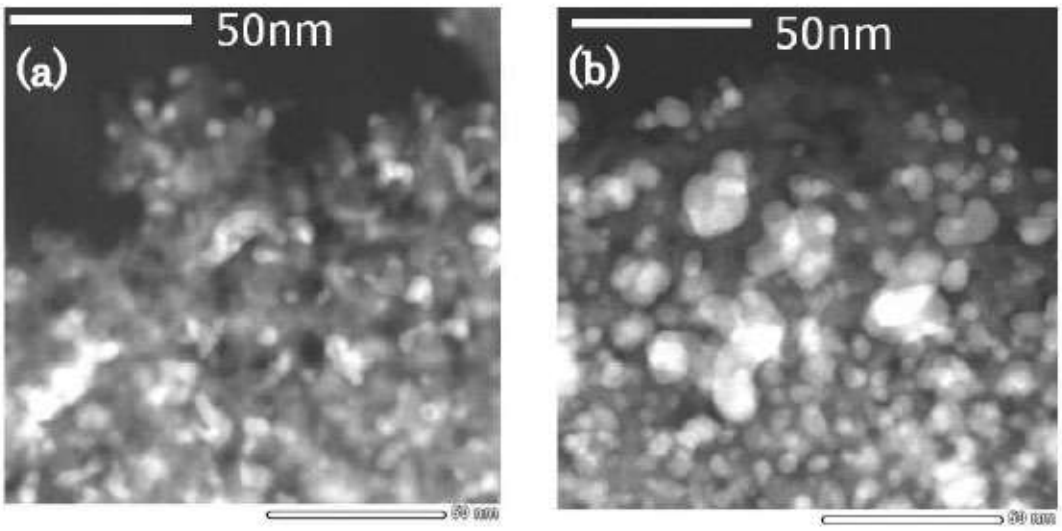

Figure 7. Scanning TEM images of 13 wt.%Pd-γAl_2O_3; (a) as-synthesized, (b) after four cycle measurements of absorption capacity. The white spots are PdO (a) or Pd (b).

3.2. Heat evolution associated with loading of hydrogen isotope gases

3.2.1. *Heat evolution during pressurizing up to 1 MPa (the first stage)*

Figure 8 shows the thermal output power as a function of time for 20 wt.%Pd-γAl_2O_3. The amount of the sample mounted in the sample vessel was 42.5 g, i.e., 8.5 g of Pd. The sample was first evacuated, heated up to 523 K, maintained at this temperature for 2 h, and cooled to room temperature. Then, the sample was loaded with deuterium. The gas pressure as a function of time is also shown in Fig. 8.

Here, we define the first stage as the period from the beginning of gas loading to the time at which the gas pressure reaches 1 MPa, the second stage as the period where the pressure is kept constant at 1 MPa. After the first measurement of heat evolution, the sample was again evacuated, heated up to 523 K, maintained at this temperature for 2 h in order to eliminate the absorbed deuterium completely. Then, the sample was subjected to the second loading with D_2 at room temperature. Similarly, the third loading was conducted with H_2. In Fig. 8, it is seen that heat evolution in the first stage is significant and especially the heat evolution in the first loading is much larger compared to those of the second and the third loadings. This behavior is quite similar to the deuterium absorption capacity shown in Fig. 5.

Therefore, the heat evolution in the first loading is related with the chemical reactions (2) and (3).

Similarly, three cycles of heat measurement were also performed for Pd powder AY4030 of 26 g. In Fig. 9, the heat generated in the first stage is summarized for both Pd powder and 20 wt.%Pd-γAl_2O_3 and compared to the values estimated from the chemical reactions (2) and (3).

For the estimation, ΔH(water) and ΔH(deuteride) were taken as -178 kJ/mol Pd [8] and -40 kJ/mol H_2 [9], respectively. It was assumed that ΔH(deuteride) $= \Delta H$(hydride). From the results of Tables 1 and 2, it was assumed that 6 at.% of Pd was initially PdO for AY4030 and 85% for 20 wt.%Pd-γAl_2O_3. In the first loading, the chemical reactions of both (2) and (3) were taken into account, in the second and the third loading only the chemical reaction (3). It is seen in Fig. 9 that the heat generated in the first stage is largely explained by the chemical reactions.

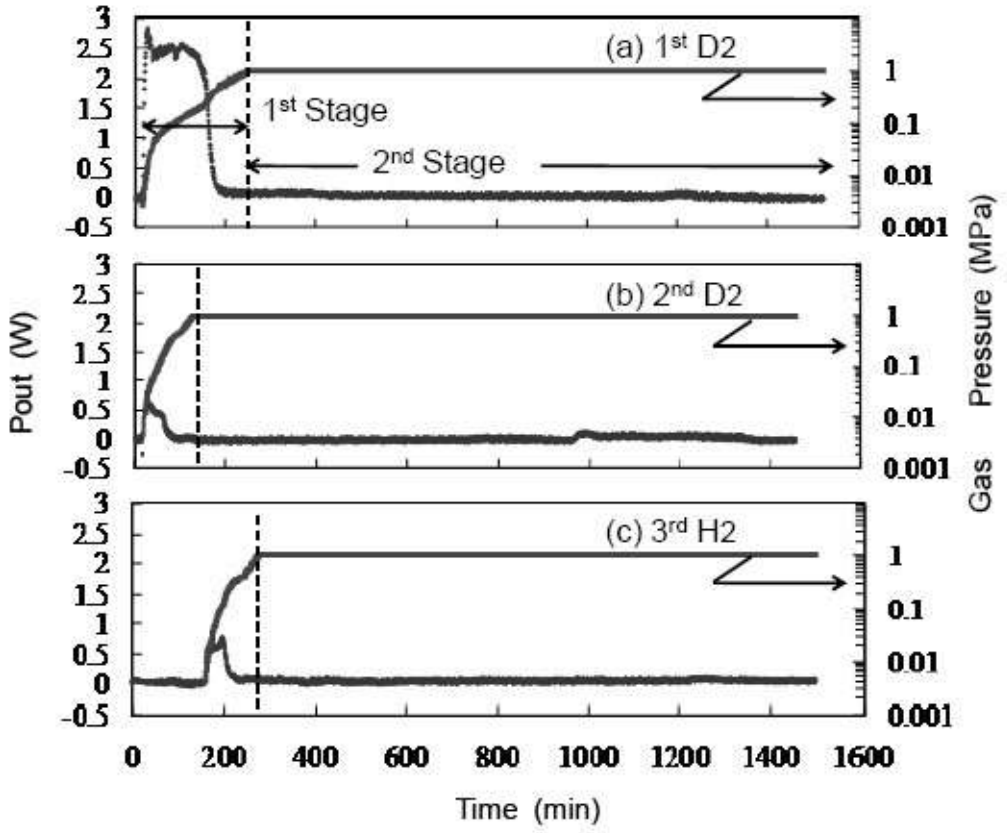

Figure 8. Heat power and gas pressure as a function of time for 20 wt.%Pd-γAl_2O_3; (a) the first cycle loading with D_2, (b) the second cycle loading with D_2, (c) the third cycle loading with hydrogen.

3.2.2. *Heat evolution under constant pressure (the second stage)*

The chemical reactions associated with loading the Pd nanoparticle systems with hydrogen isotope gases up to 1 MPa are considered to cease until the pressure reaches 1 MPa. Therefore, in the second stage where the gas pressure is kept constant at 1 MPa, no chemical reactions are expected to occur. In Fig. 10, the same data as in Fig. 8 are shown with P_{out} magnified by 10 times.

As seen in Fig. 10, in the first and the second loading with D_2, an output power as small as 0.05–0.1 W is observed for a period of about three and six hours, respectively. On the other hand, as seen in Fig. 10(c), no such anomalous heat evolution is observed in the third loading with H_2.

Similarly, the results for the Pd nanopowder sample of 26 g are shown in Fig. 11. As indicated in the figure, similar heat evolution in the second stage is also observed for the Pd nanopowder sample only under deuterium gas pressure. Therefore, it cannot be ruled out that this anomalous heat evolution in the second stage is of nuclear origin, as reported by Arata and Zhang [4] and by Kitamura et al. [6]. However, in this study, the observed anomalous heat power is as small as 0.05–0.10 W, which is close to the detection limit (±50 mW) of the calorimeter used here. Therefore, in order

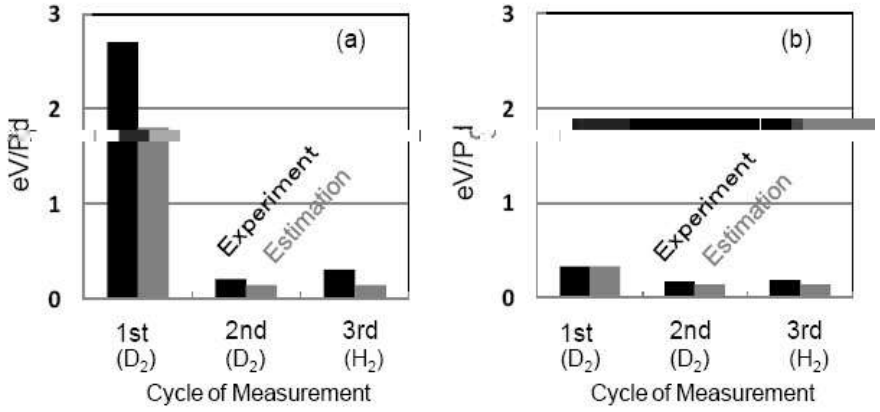

Figure 9. Variation of heat generated in the first stage with cycle of measurement for (a) 20 wt.%Pd-γAl_2O_3 and (b) Pd nanopowder AY4030. Experimental values are compared to the estimated ones.

to clarify the origin of the anomalous heat power in the second stage, it is necessary to increase the output power and/or to improve the accuracy of the calorimeter.

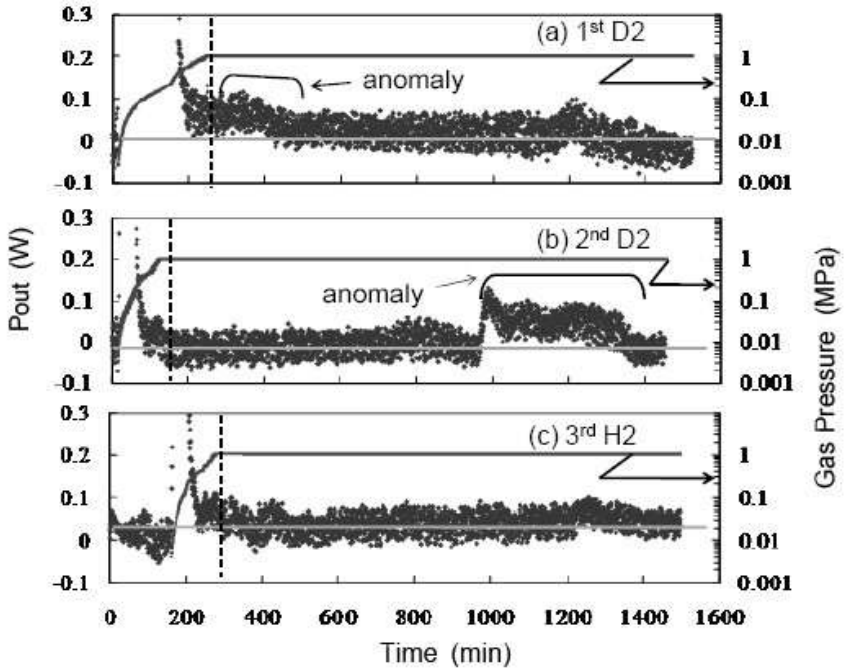

Figure 10. The same data as in Fig. 8 are displayed with the vertical axis enlarged by 10-fold. The vertical dotted lines indicate the boundary of the first stage and the second stage, and the horizontal gray lines the zero level of P_{out}.

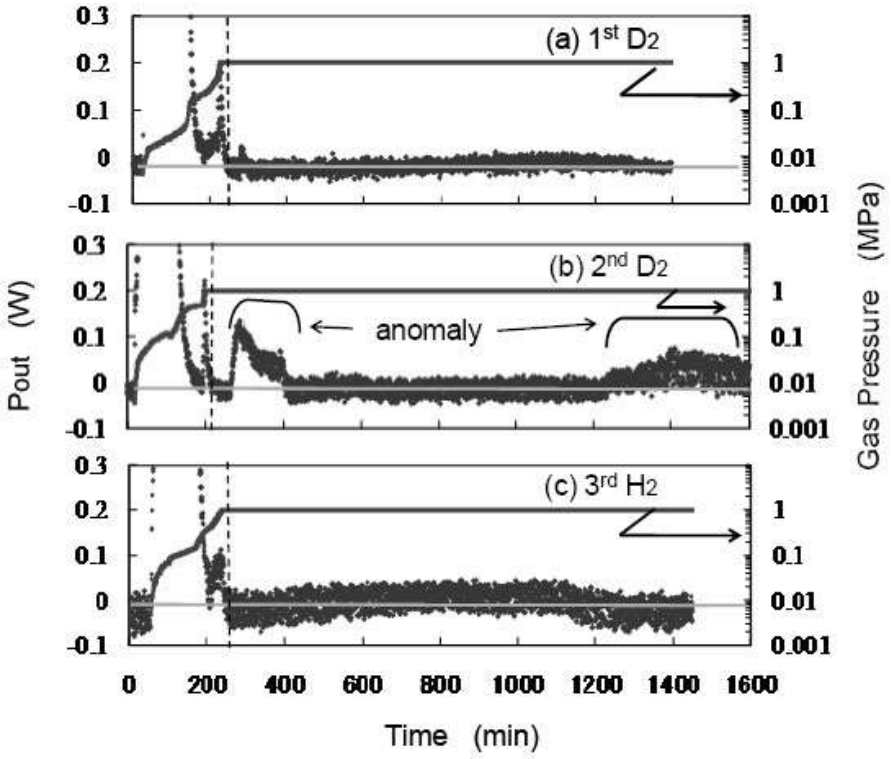

Figure 11. Heat power and gas pressure as a function of time for Pd nanopowder AY4030; (a) the first cycle loading with D_2, (b) the second cycle loading with D_2, and (c) the third cycle loading with H_2. The vertical dotted lines indicate the boundary of the first stage and the second stage, and the horizontal gray lines the zero level of P_{out}.

4. Conclusion

(1) For Pd nanoparticle systems, Pd particles are often partially or wholly oxidized, and the oxidized Pd, i.e., PdO, gives a large value of apparent absorption capacity of hydrogen isotope gases. When they are wholly oxidized, the apparent absorption capacity at 1 MPa and ambient temperature is about 2.7, which is larger than that of Pd bulk by about 3.6 times.

(2) When they are partially oxidized, the degree of oxidization, i.e., the ratio of the oxidized Pd atoms to the total Pd atoms is estimated from the difference in the apparent and the real values of the hydrogen absorption capacity.

(3) Nanoparticles of PdO were reduced to metallic Pd particles, once they were exposed to hydrogen isotope gases at ambient temperature. Therefore, if measurements of absorption capacity are performed repeatedly without exposing the sample in air, the results at the time of the second measurement give the real values of hydrogen absorption capacity for metallic Pd particles. The real values of hydrogen/deuterium absorption capacity at 1 MPa for the nano-Pd materials used in the present study were slightly smaller than that of Pd bulk.

(4) After four cyclic measurements of deuterium/hydrogen absorption capacity at 300 K, i.e., after four cycles of loading and degassing of hydrogen isotope gases, the average size of the Pd particles increased significantly compared to that of initial particles. The extent of the grain growth for the Pd nanopowder was larger than that

for the Pd-γAl_2O_3 nanocomposite.

(5) Similar to the absorption capacity, the heat generated in the first stage also depended strongly on the degree of oxidation of Pd nano-particles. The measured values of heat are largely explained by taking into account the water formation reaction and the hydride formation reaction.

(6) In the second stage, where no chemical reaction was expected to occur, an output power as small as 0.05–0.1 W was observed intermittently for a period of a few to several hours. The events of such anomalous heat generation were frequently observed for the loading with deuterium for both samples of Pd nanopowder and Pd-γAl_2O_3 nanocomposite.

Acknowledgements

We thank N. Suzuki for TEM observations, M. Hatanaka for help in preparing the materials, S. Towata, K. Aoki, T. Noritake, M. Matsumoto, and K. Miwa for discussions on hydrogen absorption capacity and for help in the measurements. Discussions on heat evolution with A. Kitamura of Kobe University and A. Takahashi of Technova Inc. were helpful. We also thank N. Nakamura of Toyota Motor Corporation for encouragement

References

[1] Y. Iwamura, M. Sakano, T. Itoh, *Jpn. J. Appl. Phys*. **41** (2002) 4642–4650.

[2] I. Dardik, T. Zilov, H. Branover, A. El-Boher, E. Greenspan, B. Khachaturov, V. Krakov, S. Lesin, A. Shapiro, M. Tsirlin, Ultrasonically-excited electrolysis experiments at energetics technologies, in Proceedings of the 14^{th} International Conference on Condensed Matter Nuclear Science, Washington DC, 2008.

[3] M. McKubre, F. Tanzella, P.L. Hagelstein, K. Mullican, M. Trevithick, The need for triggering in cold fusion reactions, in Proceedings of the 10^{th} International Conference on Condensed Matter Nuclear Science, Cambridge, Massachusetts, 2003, pp.199–212.

[4] Y. Arata, Y. Zhang, *J. High Temp. Soc*. **34** (2008) 85–93.

[5] S. Yamaura, K. Sasamori, H. Kimura, A. Inoue, *J. Mater. Res*. **17** (2002) 1329–1334.

[6] A. Kitamura, T. Nohmi, Y. Sasaki, A. Taniike, A. Takahashi, R. Seto, Y. Fujita, *Phys. Let.* A **373** (2009) 3109–3112.

[7] E. Wicke, H. Brodowsky, in *Hydrogen in Metals II*, G. Alefeld, J. Volkl (eds.), Springer, Berlin, 1978, p. 81.

[8] HSC Chemistry 6.1, Chemical Simulation and Reaction Software with Extensive Thermo-chemical Database, Outokumpu Research, Oy, Finland, 2007.

[9] Y. Fukai, K. Tanaka, Y. Uchida, Suiso to Kinzoku, Uchida Rokakuho Publishing Co. Ltd., Tokyo, 1998, p. 38 (Jpn).